CHM 696-11: Week 8

Instructor: Alexander Wei

Optical Properties of Metal Nanoparticles and Nanoparticle Assemblies

Review:

Wei, Q.; Wei, A. In *Supramolecular Chemistry of Organic–Inorganic Hybrid Materials* (Chapter 10), Mañez, R. M.; Rurack, K., Eds.; Wiley and Sons: New York, 2010; pp. 319-349

Summary on plasmon-resonant nanoparticles

1. Au and Ag nanoparticles support localized SPRs at visible and NIR wavelengths

20-nm Ag spheres: 390-400 nm; 20-nm Au spheres: 520 nm

- LSPR peaks for NPs < 5 nm are broadened, due to surface scattering (p. 6)
- LSPR peaks for NPs > 40 nm are shifted (red), due to retardation (longer e-path)

2. Metal NPs > 40 nm are strong light scatterers, detectable by eye (p.9)
   - increases with size, aggregation

3. LSPR peak shifts (red) can be due to increases in:
   - Size (p.9)
   - Aggregation (p.11)
   - Local dielectric (surface or medium) (p.14)
   - Shape anisotropy (e.g., nanorods) (p.16)

* LSPRs of anisotropic NPs are more sensitive to environmental changes than SPRs on flat surfaces or spherical NPs

Collective optical properties of NP assemblies

Models of electromagnetic coupling between particles: large shift in collective SPR

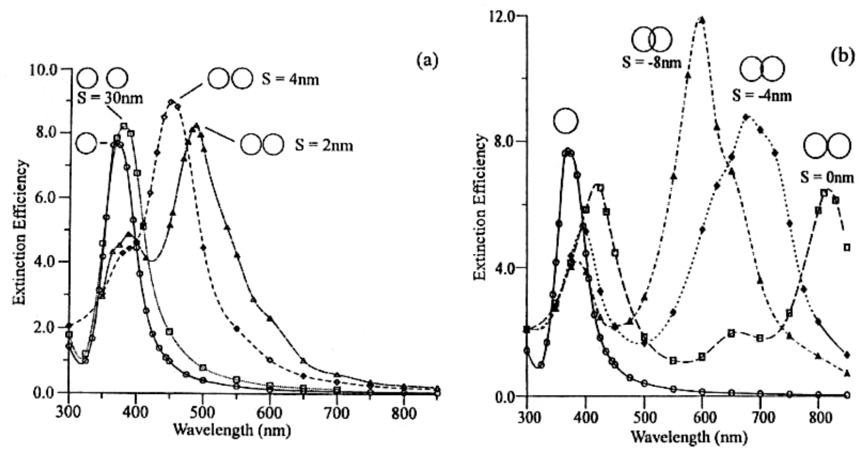

Discrete dipole approximation (DDA) of 30-nm Ag particle dimer as a function of separation (S)

Jensen et al, *J. Cluster Sci.* **1999**, *10,* 295.

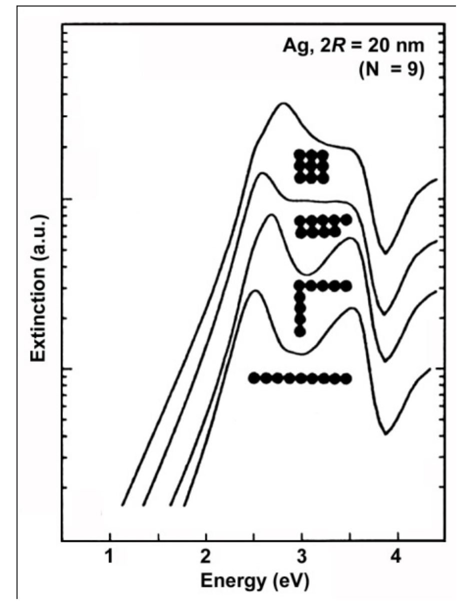

Simulation of (GMT) collective SPR of Ag NPs assembled into different geometries

Kriebig and Vollmer, *Optical Properties of Metal Clusters,* 1995.

<u>Challenges in comparing experiment and theory</u>:

- calculations for particle sizes greater than 40 nm (quasistatic limit)
- Strong, highly nonlinear plasmon coupling between <u>closely</u> spaced particles (< 50% of diameter)
- Accounting for structural or surface charge defects ; establishing local dielectric constants (ε_d)

Optical properties of 2D metal nanoparticle arrays

2D arrays of small (< 10 nm) Ag NPs (nanoparticle superlattices)

Alkanethiol-coated 2.7-nm Ag nanoparticles self-organized into 2D hexagonal close-packed (hcp) arrays at the air-water interface, then transferred onto a carbon-coated TEM grid

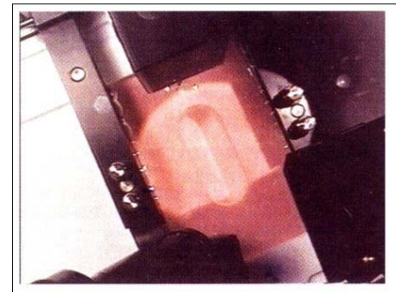

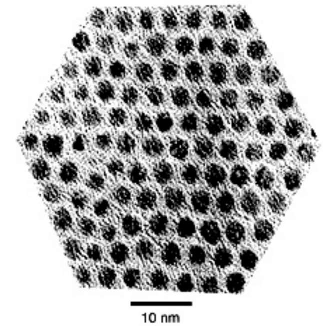

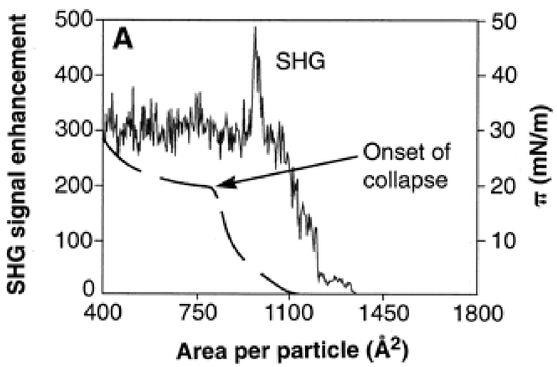

Exponential rise in second-harmonics generation (SHG) with reduced interparticle spacing (compression), for $D/2R$ between 1.7 and 1.2

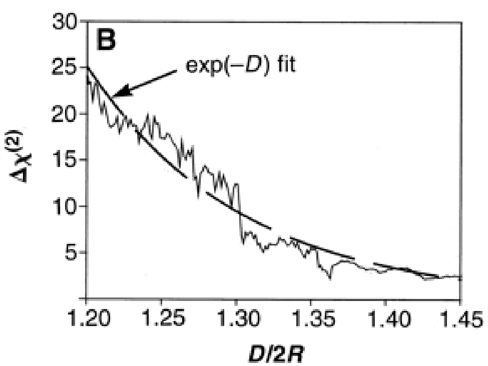

Loss of SHG, reflectance when $D/2R < 1.2$; onset of quantum-mechanical coupling between nanoparticles

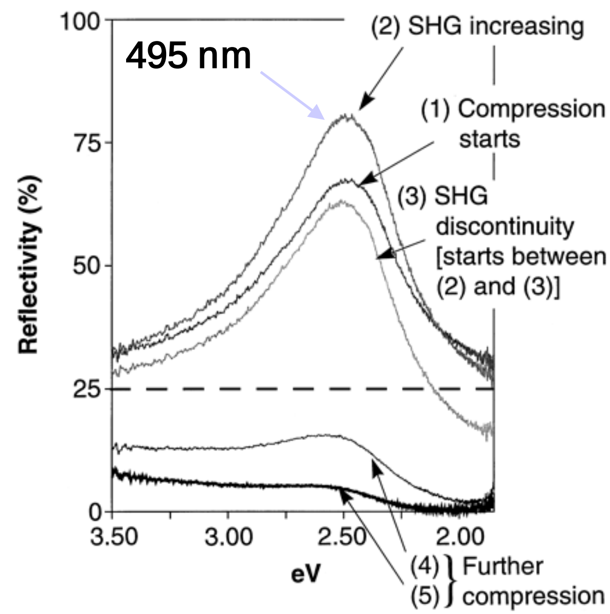

D = center-to-center spacing ($2R$+S)

Collier et al, *Science* **1997**, *277*, 1978.
Markovich et al., *Acc. Chem. Res.* **1999**, *32*, 415.

Optical properties of 2D metal nanoparticle arrays

2D arrays of large (> 10 nm) Au NPs

Calixarene-coated Au nanoparticles: self-assembly into 2D close-packed arrays at the air-water interface, then transferred onto substrates

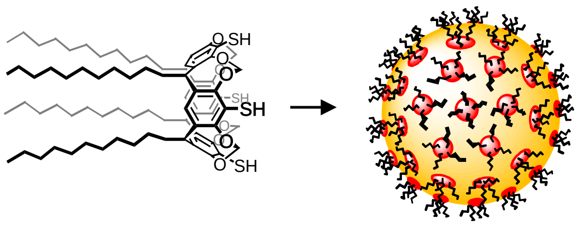

Resorcinarene tetrathiol

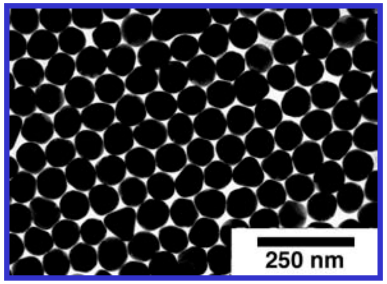

2D array of 87-nm Au nanoparticles

Collective SPR of 2D nanoparticle arrays
(λ_{max}: 624 ~ 1050 nm)

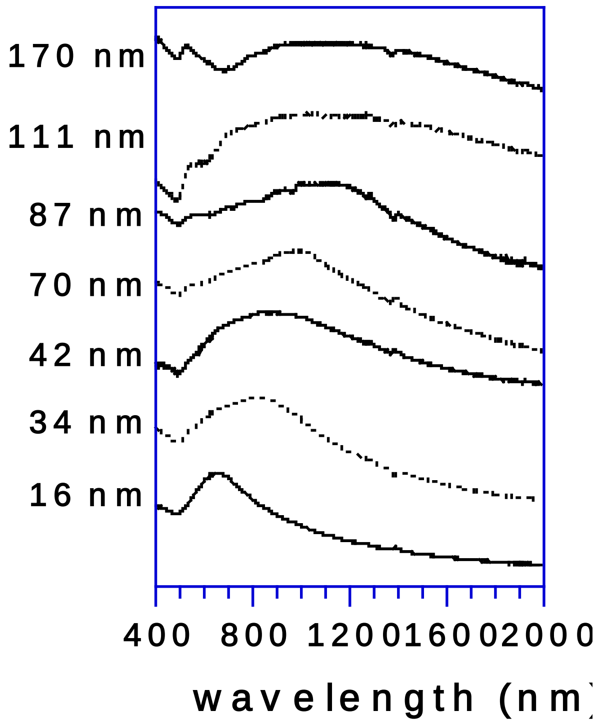

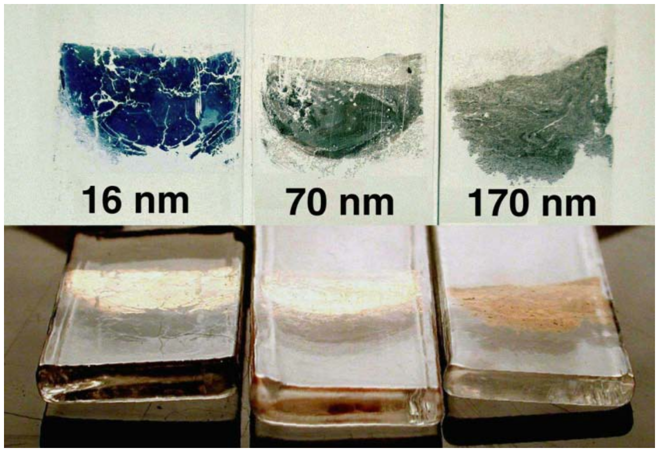

Kim, Tripp, and Wei, *J. Am. Chem. Soc.* **2001**, *123*, 7955.
Wei et al. *ChemPhysChem* **2001**, *2*, 743.

Plasmon-enhanced field effects

Origin of plasmon-amplified signals in surface-enhanced Raman scattering (SERS) and other optical emissions

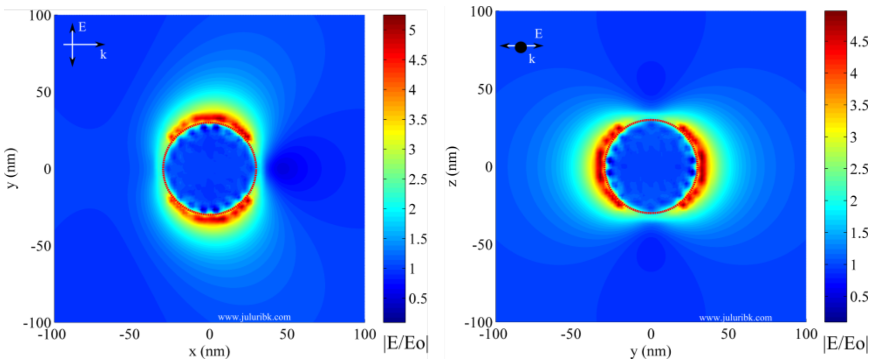

Local EM field factors (E/E_0):
extends for several nanometers from NP surface, in direction of LSPR mode

EM field factors in NP assemblies:

Local field factors increase nonlinearly as a function of particle <u>diameter–spacing ratio (γ)</u>

Size of ensemble, unit particle size are also important factors in EM enhancement

Calculation of $G = (E/E_0)^4$ in Ag NP dimer, as a function of interparticle separation

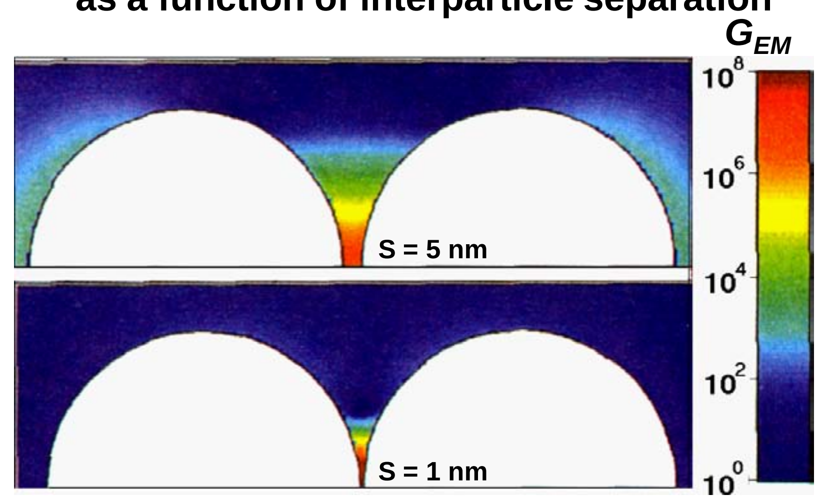

λ_{ex}=514.5 nm; $2R$ =90 nm, S= 1 or 5 nm (Ag)

Xu et al, *Phys. Rev. E* **2000**, *62*, 4318.

Plasmon-enhanced emissions

A. Surface-enhanced Raman scattering (SERS)

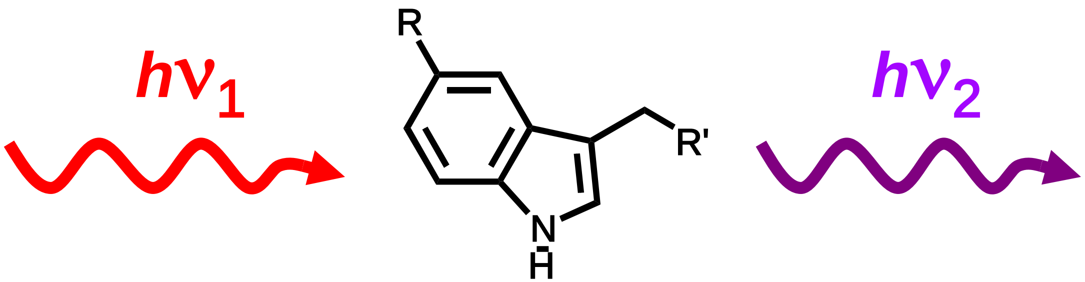

analyte

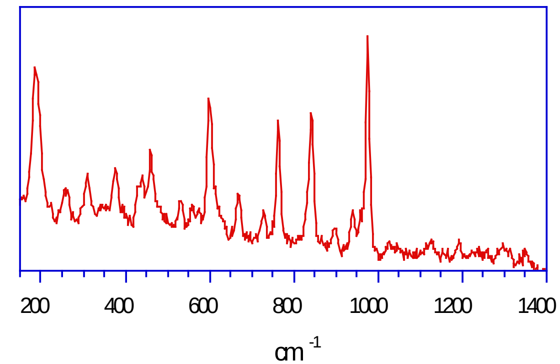

Raman spectrum

nanostructured Ag and Au surfaces
(roughness ~ 10-200 nm)

- Label-free chemical sensing
- Multiplexing capabilities
- Water is Raman-silent
- relationship between nanostructure and activity often not well-defined
- SERS-active substrates are easy to make, but can be tricky to reproduce

“Hot Spots” in SERS-active substrates

SERS activity is strongly correlated with local electromagnetic (EM) field factors

“Hot spots” can be found at edges and tips of anisotropic NPs, but can be even stronger in gaps between closely spaced metal nanostructures

SERS-active “nano-crescents”

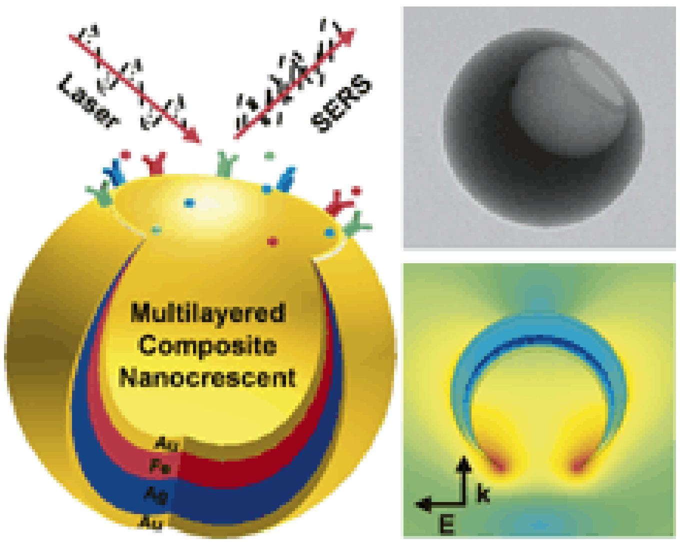

Liu et al. *Adv. Mater.* **2005**, *17*, 2683.

Self-assembled Au nanoparticle arrays

2D array of 87-nm Au NPs

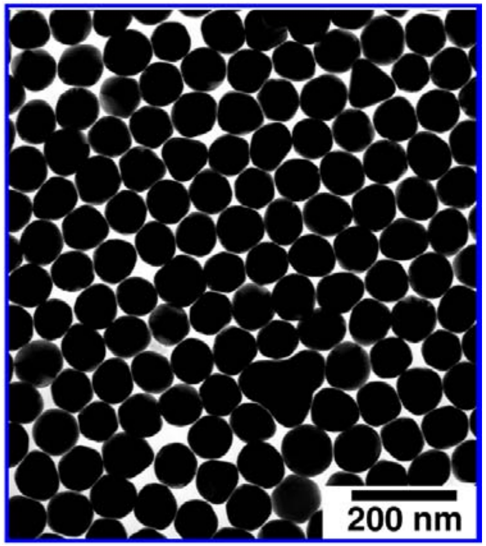

Wei et al, *ChemPhysChem* **2001**, *2*, 743.

λ_{ex}=647 nm; γ = 5 or 10 (Au)

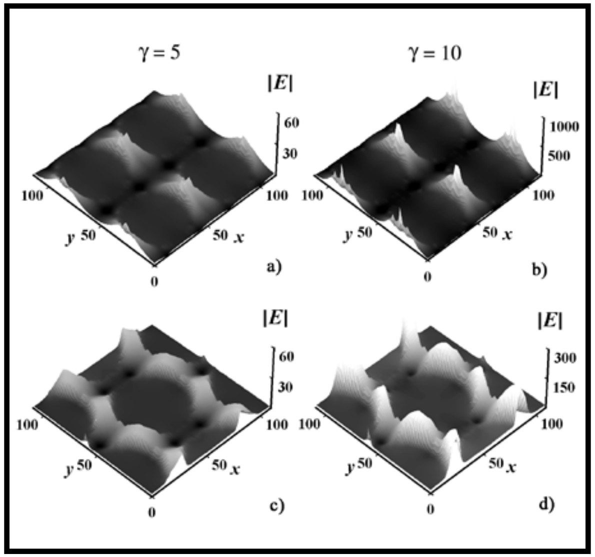

Genov, Sarychev, Shalaev, Wei, *Nano Lett.* **2004**, *4*, 153.

Plasmon-enhanced emissions

B. Surface-enhanced fluorescence (SEF)

Highly sensitive to distance between fluorophore and metal surface: SEF also relies on local EM field factors, but excited states can be quenched by back-electron transfer

Nanometric coatings for optimizing SEF (up to 20-fold increase in fluorescence)

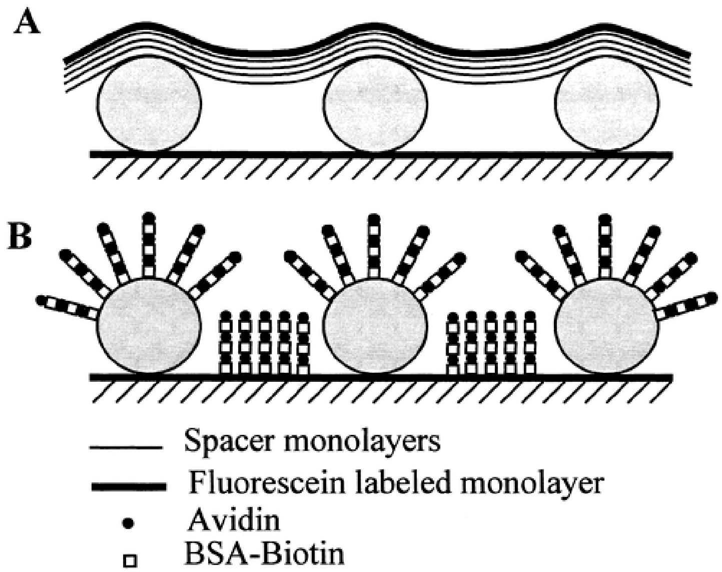

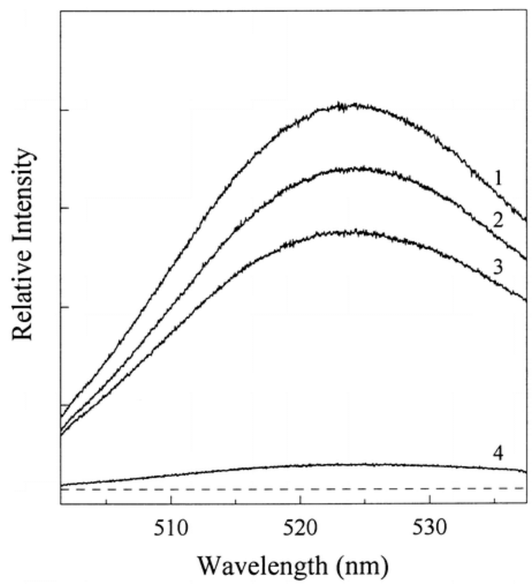

Sokolov, Chumanov, and Cotton, *Anal. Chem.* **1998**, *70*, 3898.

← No SEF

Multilayers of phospholipid or BSA−biotin/avidin over Ag NPs, then coated with fluorophore

Fluorescence intensity of biotin−FITC on top of (1) six, (2) four, and (3) two monolayers formed by alternating avidin and BSA−biotin.

Plasmon-enhanced emissions

C. Förster resonance energy transfer (FRET)

Energy transfer mediated by overlap between emission and absorption (donor−acceptor) bands; D−A distance <10 nm

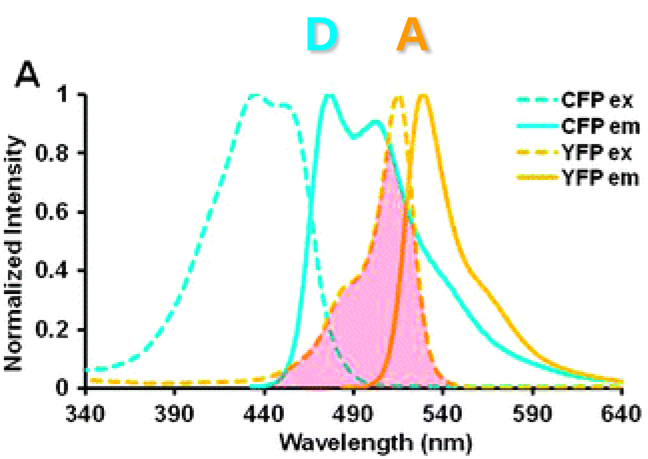

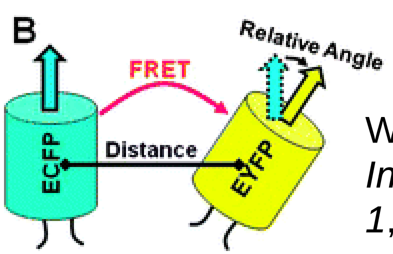

Wang and Wang, *Integr. Biol.* **2009**, *1*, 565

Plasmon-enhanced FRET: greater efficency and range

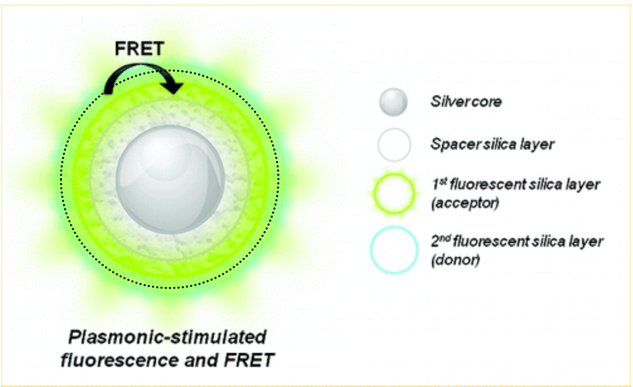

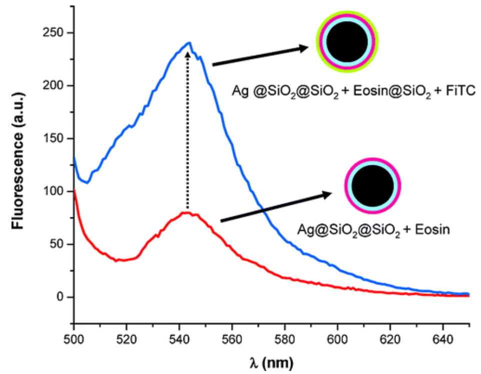

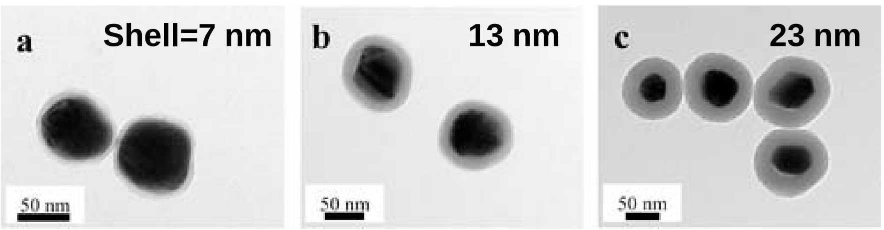

Dye-doped Ag@SiO$_2$ core-shell NPs

Lessard-Viger et al, *Nano Lett.* **2009**, *9*, 3066.

Imaging: Metal NPs as optical contrast agents

A. Resonant light scattering: Darkfield microscopy

Plasmon-resonant NPs used as biological imaging labels must also compete with other scatterers.

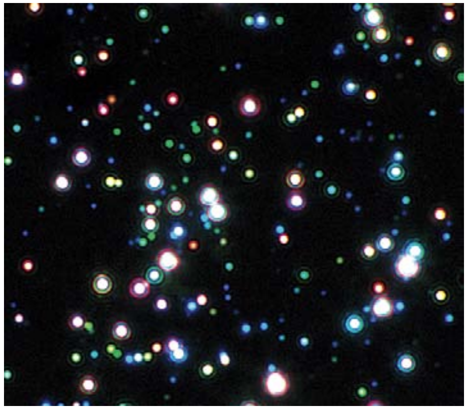

Ag nanoparticles of variable size and shape

Cross-polarized scattering: a novel method of noise reduction for anisotropic NP labels

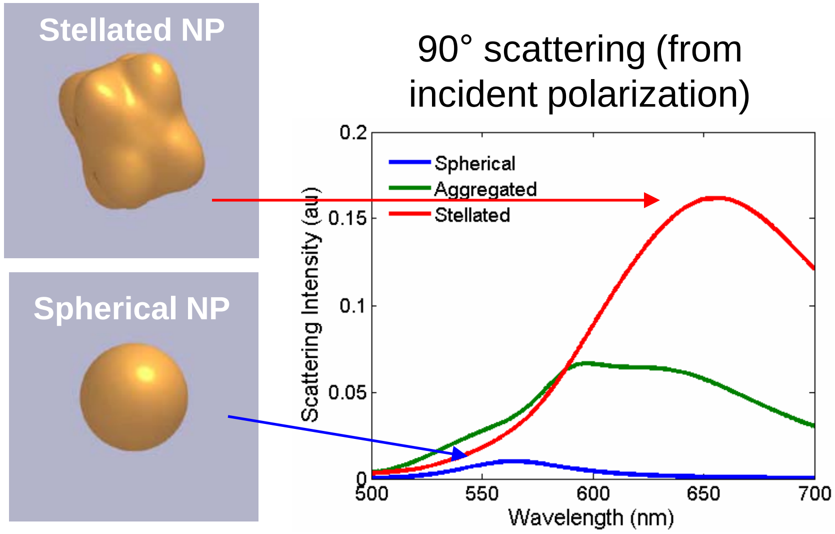

A431 cells with anti-EGFR labeled nanostars

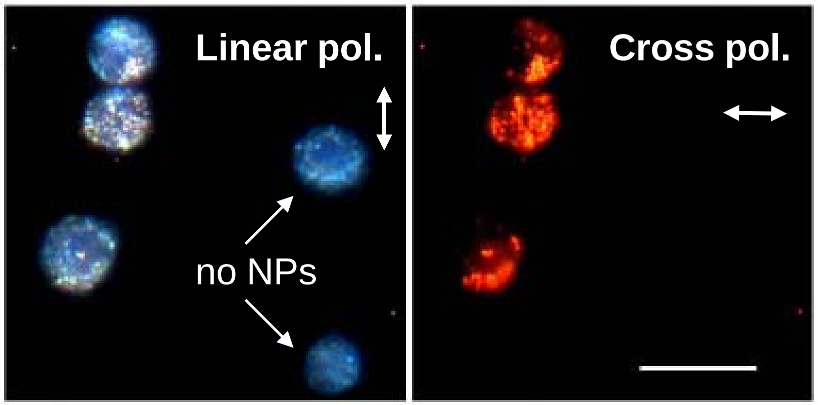

Aaron et al, *Opt. Express* **2008**, *16*, 2153.

Imaging: Metal NPs as optical contrast agents

B. Multiphoton excitation

Two-photon excited luminescence (TPL) from Au nanorods

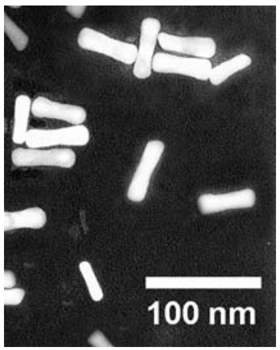

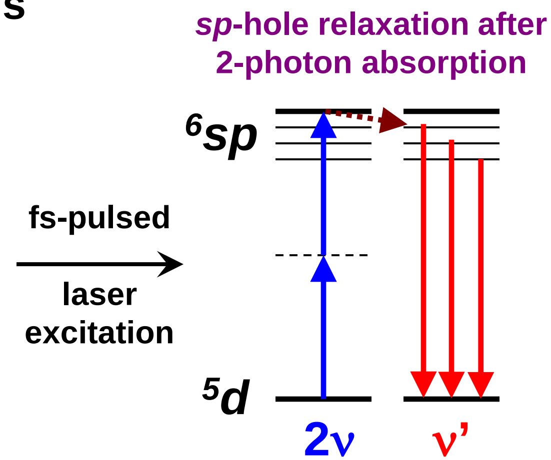

TPL intensity vs. Au NR absorption:

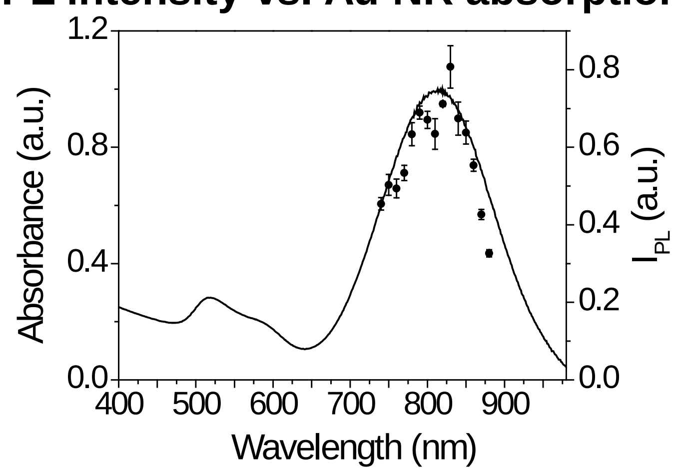

TPL of Au NRs on glass slide

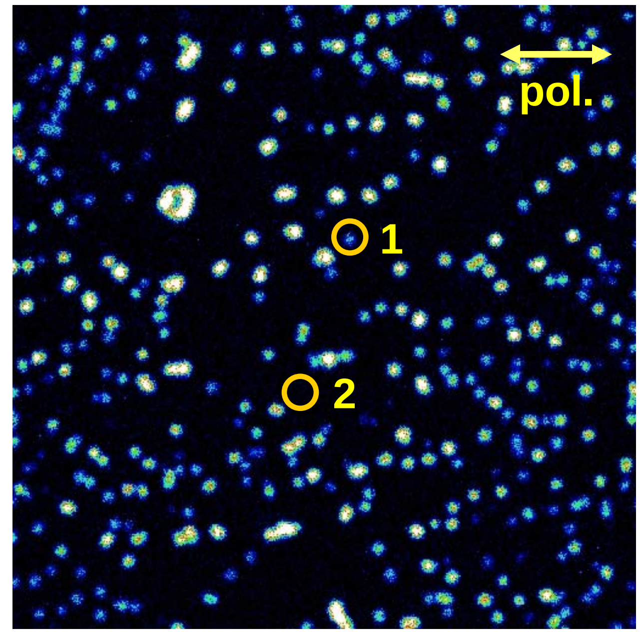

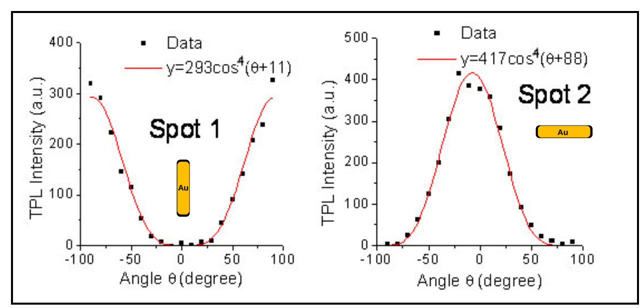

Wang *et al*. *PNAS* **2005**, *102*, 15752.

Multiphoton imaging has very low autofluorescence

In vitro **TPL imaging of Au NR uptake by KB cell: single-particle sensitivity**

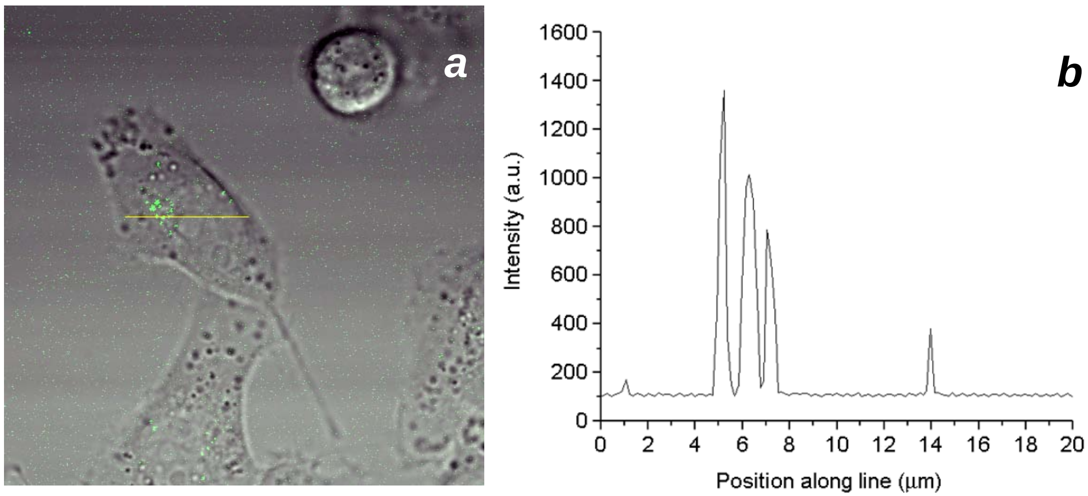

(a) TPL image of Au NRs (green) internalized by KB cells after a 5-hour incubation (linescan = 75 µm).

(b) Intensity profile across yellow linescan in (a); high SNR provided by TPL contrast.

Huff et al, *Nanomedicine* **2007**, *2*, 105.

In vivo **TPL imaging of Au NRs flowing through blood vessel in mouse ear**

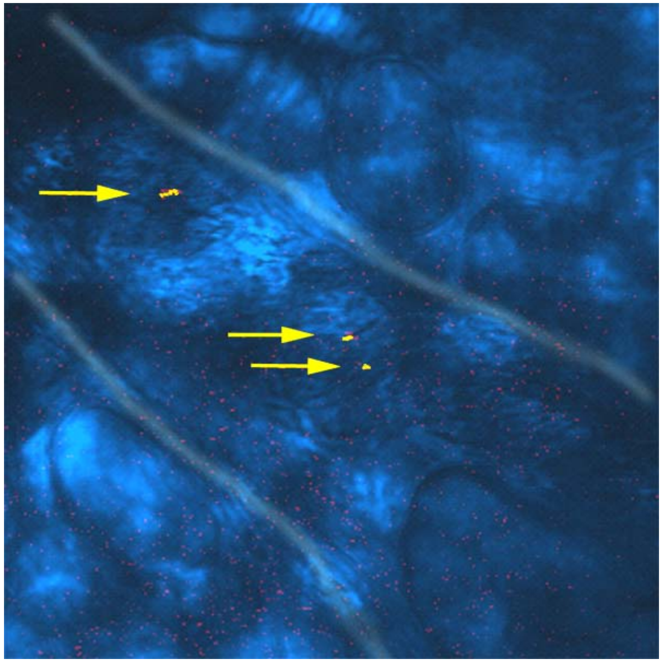

Wang *et al*. *PNAS* **2005**, *102*, 15752.

Imaging: Metal NPs as optical contrast agents

C. Au NPs as SERS tags

in vitro detection of labeled SERS tags: compares well with fluorescence imaging

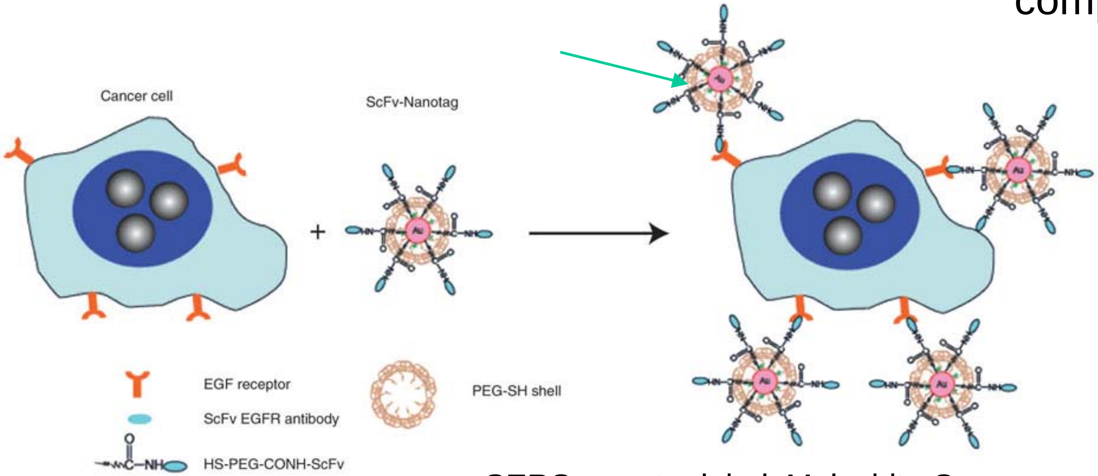

SERS reporter label: Malachite Green

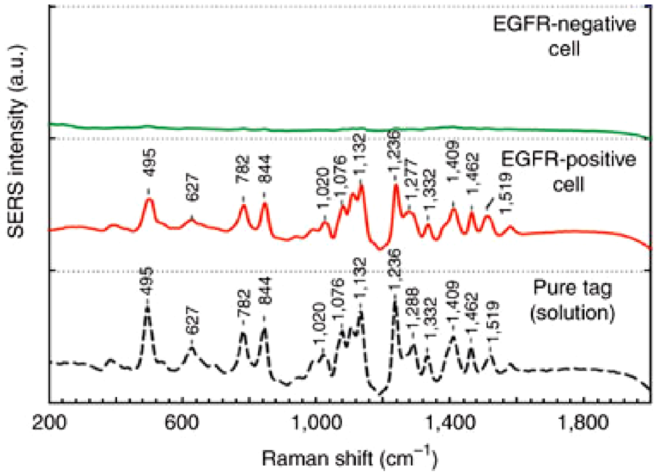

Targeted *in vivo* delivery of SERS labels to tumor in nude mouse model:

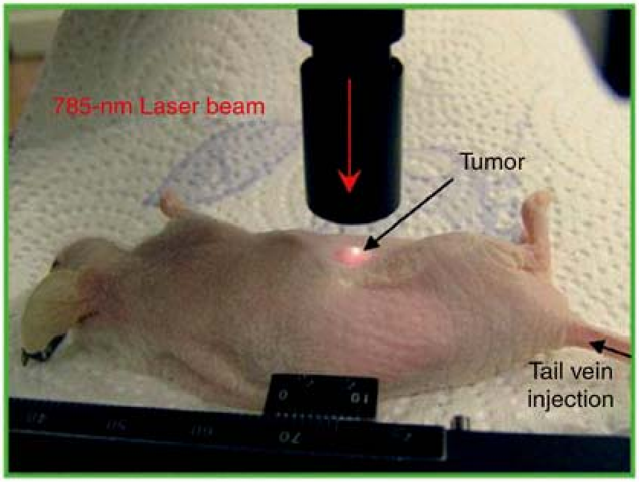

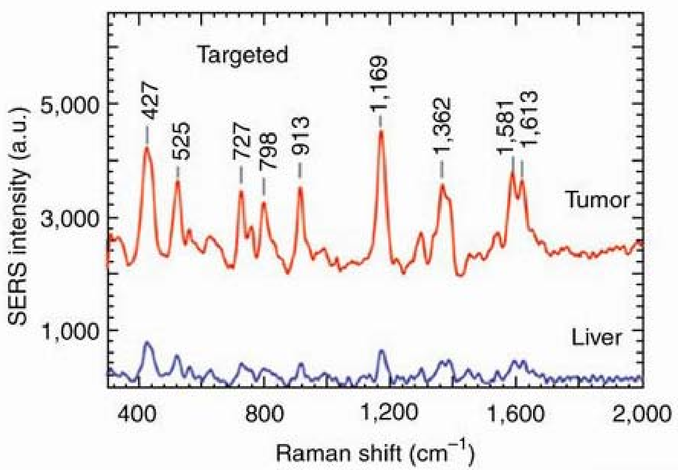

Qian et al, *Nat. Biotechnol.* **2008**, *26*, 83.

Imaging: Metal NPs as optical contrast agents

D. Other optical modalities for biomedical imaging

Optical coherence tomography

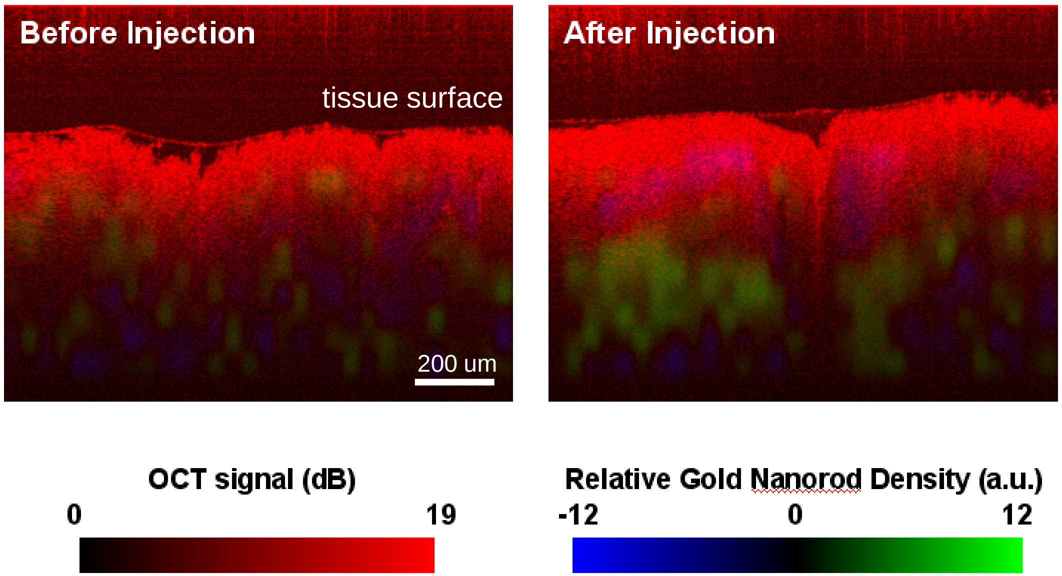

OCT contrast by Au NRs in human breast carcinoma tissue

Oldenburg et al, *J. Mater. Chem.* **2009**, *19*, 6407.

Eghtedari et al, *Nano Lett.* **2007**,*7*, 1914.

Photoacoustic tomography

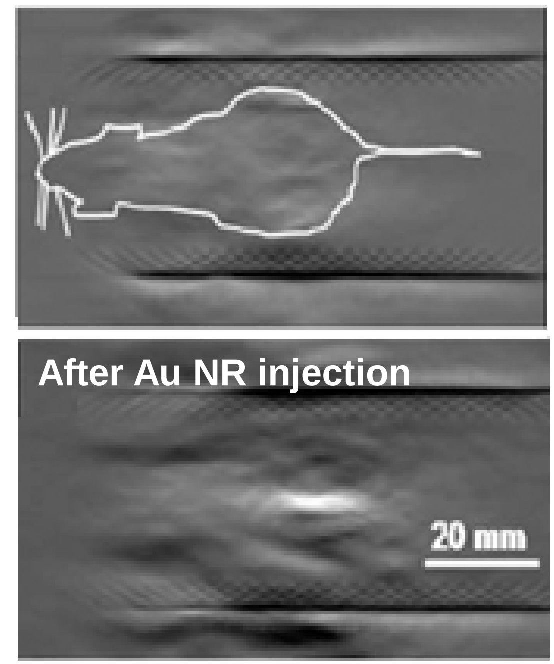

PAT of Au NRs within nude mouse (before and after injection)

Relatively high loadings of Au NPs are still required to generate sufficient contrast in tissue for these imaging modalities.

Hybrid magnetic-plasmonic nanoparticles

Dynamic contrast (gyromagnetic imaging) from NIR-resonant Au nanostars with magnetic cores:

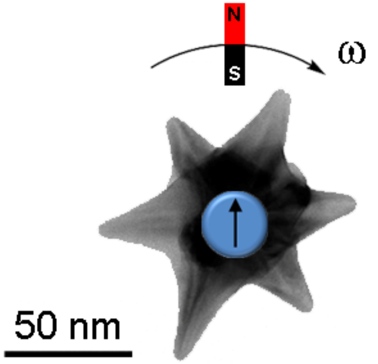

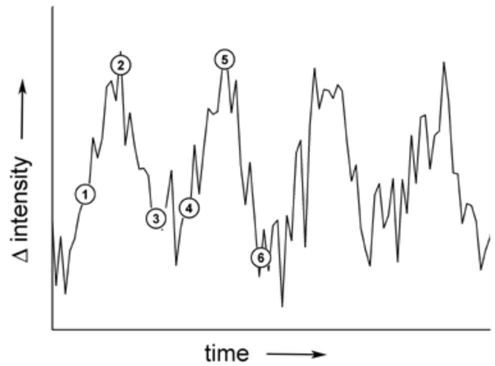

polarized scattering from single nanostar (in real time)

FFT →

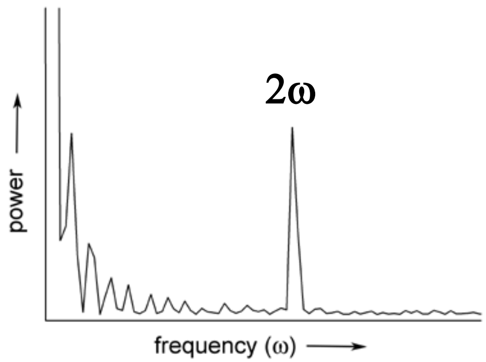

Power density spectrum with freq.-selective signal at 2ω

Nanostars in KB cell: frequency-selective filtering for noise reduction

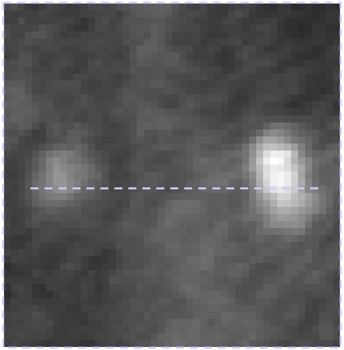

Time-domain (left signal): **15.9 dB**

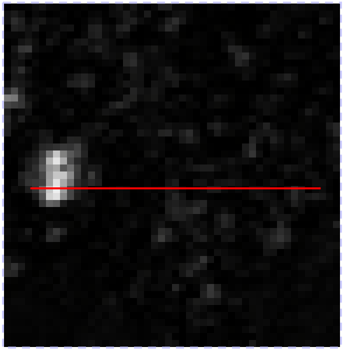

Fourier-domain signal: **28.1 dB**

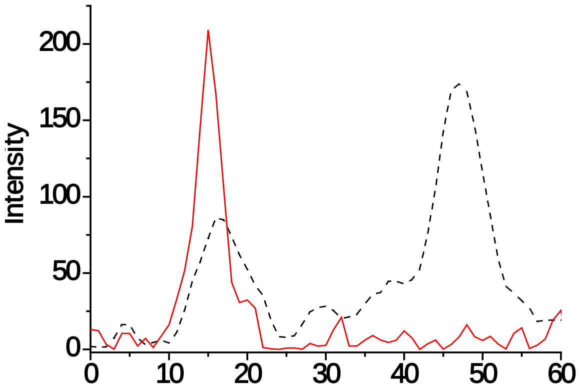

Wei et al, *J. Am. Chem. Soc.* **2009**, *131*, 9728.

Photothermal activity of metal nanoparticles

Absorbed light is mostly converted into heat

Estimation of surface temperature on Au NP:

$$\Delta T = \frac{E_{abs}}{mc_p}$$

ΔT for 5-nm Au sphere =15 K at LSPR saturation

E_{abs} =absorbed photon energy
m =mass of Au NP
c_p = heat capacity of Au

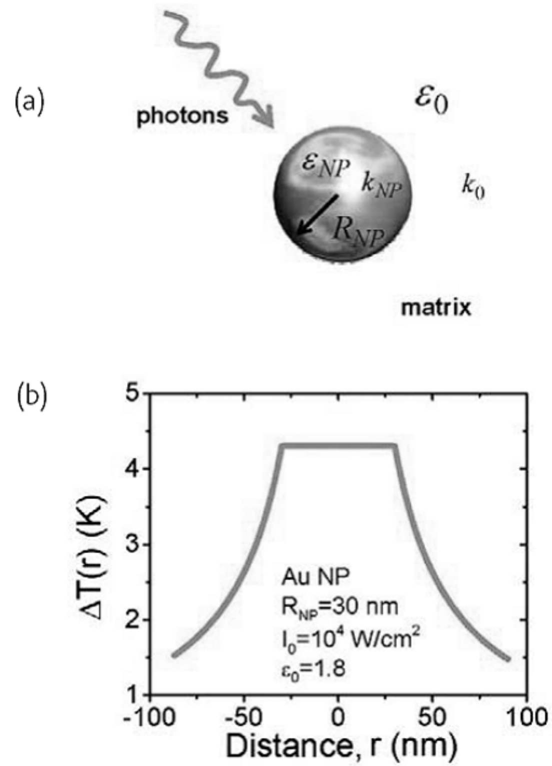

Estimation of heat transfer to environment of Au NP:

$$\Delta T(r) = \frac{V_{NP} Q}{4\pi k_0 r}$$

1/*r* dependence

V_{NP} = volume of NP
Q = heat of NP
k_0 = thermal conductivity of medium
r = distance from surface

Govorov and Richardson, *Nano Today* **2007**, *2*, 30.

Photothermal activity of metal nanoparticles

Timescale of photothermal response, induced by pulsed laser excitation:

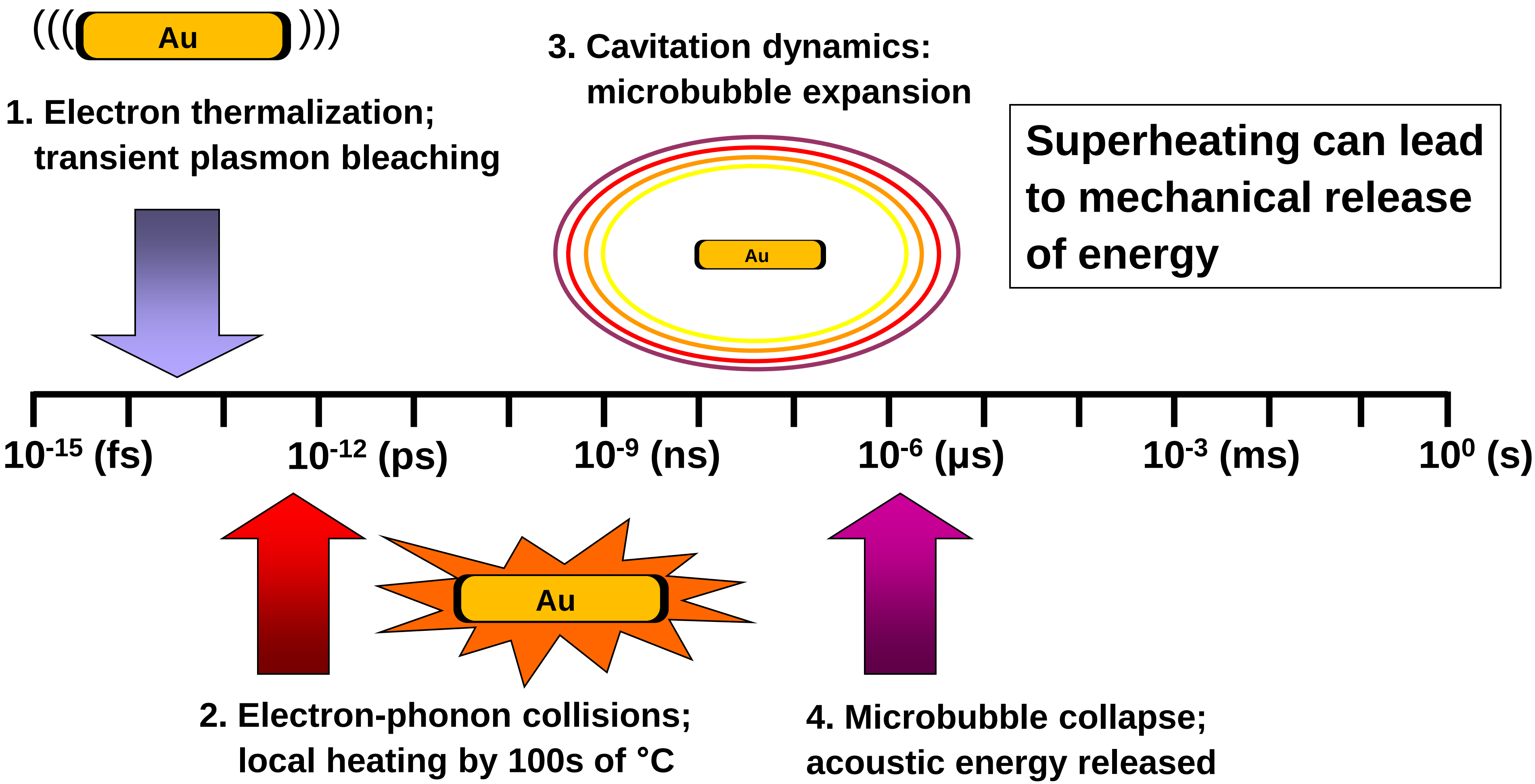

Link and El-Sayed, *Int. Rev. Phys. Chem.* **2000**, *19*, 409.
Pitsillides et al, *Biophys. J.* **2003**, *84*, 4023.

Photothermolysis of tumor cells mediated by Au NRs targeted to cell membranes

Membrane-bound Au NRs on tumor cells

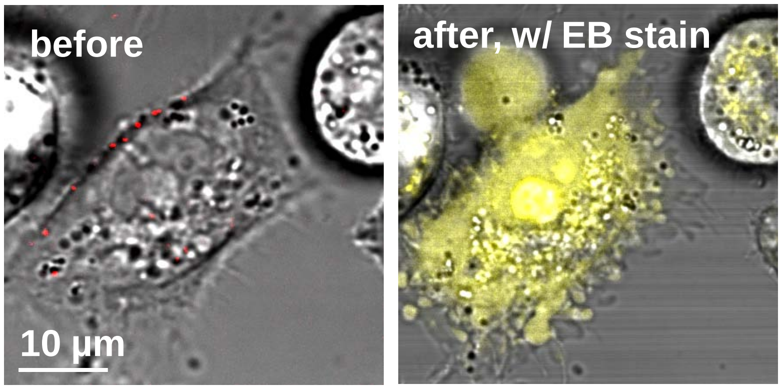

81 s scan, cw mode:
Laser power = 6 mw; fluence = 24 J/cm^2

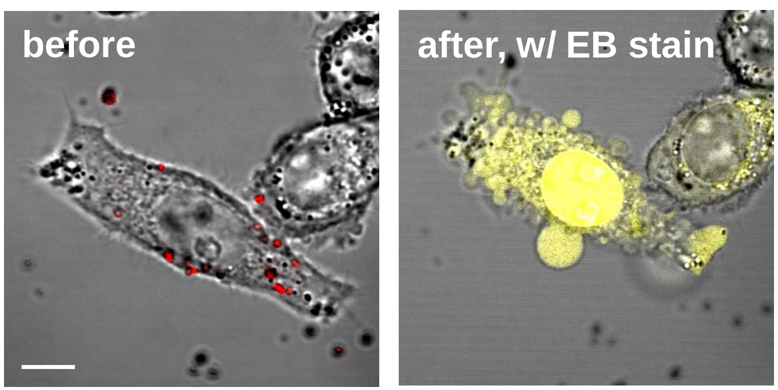

81 s scan, fs-pulsed mode:
Laser power = 0.75 mw; fluence = 3 J/cm^2

Internalized Au NRs

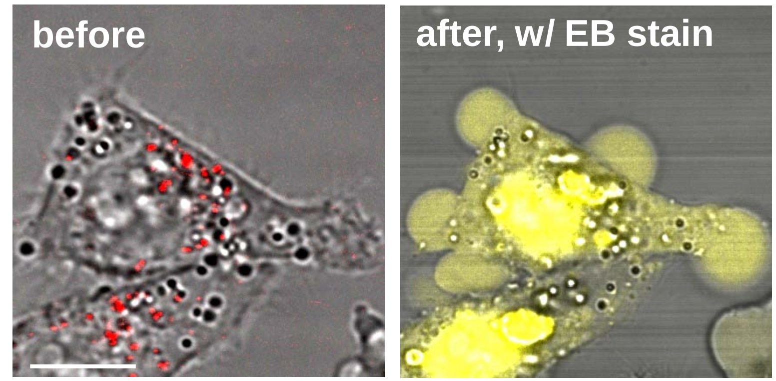

81 s scan, cw mode:
Laser power = 60 mw; fluence = 240 J/cm^2

Threshold fluence for hyperthermic damage (blebbing) is 10X lower or more when nanorods are localized on cell membranes

Tong et al, *Adv. Mater*. **2007** *19*, 3136.